Harmonics of S motion on bowed strings

Bo Lawergren
Hunter College of the City University of New York, 695 Park Avenue, New York, New York 10021

(Received 3 February 1981; accepted for publication 10 March 1983)

Lossless bowed strings have usually been thought to possess a motion discovered by Helmholtz in 1863. However, it was shown [Acustica **44**, 194–206 (1980)] by the author that a more complicated standing wave motion, the S motion, exists on such strings provided both the bowing distance and bowing force are above certain minimum values. This paper explores S-motion harmonics which give arise to waveforms of considerable complexity on very thin strings. Equations are found which describe the experimentally determined waveforms as a function of bow position, bow velocity, and observation point. In the special case of square velocity waves at the bow point, the equations give quantized values for the bow/string sticking duration. That result agrees with Raman's [Proc. Ind. Assoc. Adv. Sci. **15**, 1–158 (1918)] prediction. In general, however, the waveforms have rounded corners.

PACS numbers: 43.75.De

INTRODUCTION

Earlier[1,2] we have described studies of violin strings bowed on a monochord. The general transverse motion of a lossless string was found to be different from that described by Helmholtz.[3] We derived an expression which accounted well for the motion provided the bowing point lay more than 5 cm from the bridge on a normal violin string (33 cm long) and the downward bowing force on the string exceeded a certain minimum value (the critical force). In essence, the motion expression consisted of a prominent sinusoidal component (S motion) superposed on the Helmholtz[1] motion. The period of the sinusoid is β (β is defined below). Permanent node points existed at the two ends of the string and a temporary, intermittent, node occurred at the bow. The expression was chosen to give continuity at the bowing point (in position and spatial derivative). This choice led to an inverse relationship between bowing position and S-motion velocity amplitude. The fact that S motion is not observed for small bowing distances can then be understood, at least qualitatively: the bow is unable to sustain the large kinetic energy resulting from the S-motion amplitudes.

During the time interval a the transverse velocity was found to be

$$v = v_0\left(\frac{\cos(2\gamma\tau)\sin[(1-\delta)\gamma]}{\beta\sin\gamma} - \frac{1-\delta}{\beta}\right) \tag{1a}$$

and during time interval b,

$$v = v_0\left(\frac{\delta}{\beta} - \frac{\cos[(\tau-0.5)2\gamma]\sin(\delta\gamma)}{\beta\sin\gamma}\right). \tag{1b}$$

v_0 is the velocity of the bow (in absolute units).

β is the dimensionless bow position, i.e., the ratio of the length L_b between the bridge and the bow point and the total length L of the string; $0<\beta<1$.

δ is the dimensionless observation distance, i.e., the ratio of the length L_0 between the bridge and the point of observation and the length L; $0<\delta<1$.

γ is π/β.

τ is the dimensionless time variable, i.e., the ratio of the time and the duration of the fundamental period of the oscillating string; $0<\tau<1$.

Interval a is $-\delta/2<\tau<+\delta/2$ and interval b is $+\delta/2<\tau<(1-\delta/2)$. (Intervals a and b denote regions in the space–time diagram for traveling waves on the string as illustrated in Fig. 15a, Ref. 1.)

As mentioned above, these expressions apply when $\beta>0.18$ and the bowing force exceeds the critical force. The critical force varies inversely[4] with β from a low value of 0.05 N at $\beta=0.36$ to 0.4 N at $\beta=0.18$.

As with other standing-wave phenomena, the S motion must possess upper partials of its fundamental mode. Such modes of vibration should be characterized by $(n-1)$ nodes between the bridge and the bowing point. This paper deals with the form of these modes and their occurrence on real strings as well as on ideal strings. The latter topic connects harmonic S motion to Raman's theory of bowed string motion.[5]

I. APPARATUS

Expression (1) was derived from velocity waveforms recorded at several positions along the string. The records had to be measured at constant bow velocity, bow position, and bow force. For this purpose a bowing machine was developed. A violin bow ran on horizontal tracks pulled by a servo controlled, printed armature, motor[6] which automatically alternated up- and down-bow strokes and kept a constant bow velocity of 9 cm/s. The bow hairs were squeezed to a 4-mm-wide bundle but, otherwise, the bowing conditions were similar to those in a normal violin. The monochord rested on a platform with adjustable height. The downward force on the monochord could be monitored by means of strain gauges. In order to bring out the different modes of vibration, we used a thin string of "rocket wire"[7] with 0.16-mm diameter and 0.2-g/m mass. It had a length of 33 cm and frequency of 440 Hz. The string passed through the vertical field of a permanent magnet and the induced signal was fed

 0001-4966/83/062174-06$00.80

to a waveform recorder[8] for off-line plotting and analysis in the time domain.

II. HARMONICS OF THE *S* MOTION

For normal violin strings harmonics of the S motion are, essentially, damped out and Eq. (1) adequately describes the motion ("normal S motion"). However, our experimental data show that Eqs. (2) and (3) must be used to describe the motion of thinner strings. For transverse deflection

$$d = \sum_{n=1}^{\infty} d(n), \tag{2}$$

$$d(n) = \left(\frac{v_0}{f}\right) F(n)\left(\frac{\sin(2\gamma\tau n)\sin[(1-\delta)\gamma n]}{2\pi\sin(\gamma n)} - \frac{1-\delta}{\beta}\tau\right), \tag{2a}$$

$$d(n) = \left(\frac{v_0}{f}\right) F(n)\left(\frac{\delta(\tau-0.5)}{\beta} - \frac{\sin[2\gamma n(\tau-0.5)]\sin(\gamma\delta n)}{2\pi\sin(\gamma n)}\right), \tag{2b}$$

and Eq. (3) for transverse velocity[9]

$$v = \sum_{n=1}^{\infty} v(n), \tag{3}$$

$$v(n) = v_0 F(n)\left(\frac{\cos(2\gamma\tau n)\sin[(1-\delta)\gamma n]}{\beta\sin(\gamma n)} - \frac{1-\delta}{\beta}\right), \tag{3a}$$

$$v(n) = v_0 F(n)\left(\frac{\delta}{\beta} - \frac{\cos[2\gamma n(\tau-0.5)]\sin(\gamma\delta n)}{\beta\sin(\gamma n)}\right). \tag{3b}$$

Equations (1a), (2a), and (3a) apply in the same interval as do Eqs. (1b), (2b), and 3(b), respectively. $F(n)$ is the amplitude of the nth mode and f is the frequency of the fundamental string vibration. The F factors must be normalized to make the infinite sum $\Sigma F(n) = 1$. As required, the harmonics are characterized by additional temporary nodes with spacings equal to the distance between the bow and the bridge divided into n equal segments. These nodes exist only during the sticking period. String shapes and waveforms created by the addition of S-motion harmonics as in Eqs. (2) and (3) have the same continuity properties as in Eq. (1) discussed previously.[1]

Harmonic S motion can lead to vastly more complex waveforms than normal S motion. Figure 1 shows a set of thin-string measurements at a bowing position of $\beta = 0.418$. Five terms in Eq. (3) [$F(1) = 1.7$; $F(2) = -1.3$; $F(3) = 1.0$; $F(4) = -0.7$; $F(5) = 0.3$] were needed to give the fit in Fig. 1. These waveforms are more difficult to match with Eq. (3) than previous measurements[1] because the present data are more highly dependent on the bowing position and the observation points (the nodes are more closely spaced) and somewhat dependent on the bow force (which must exceed the critical values for each relevant harmonic). There are no adjustable parameters in normal S motion but in harmonic S motion the amplitudes $F(n)$ are arbitrary. With this in mind, the data of Fig. 1 lend reasonable support to the predictions of Eq. (3).

Often (but not always, as can be seen in Fig. 6) harmonic motion requires higher critical bow force than normal S motion. The dependence of S motion amplitude on the bow force, qualitatively, resembles the behavior of normal mo-

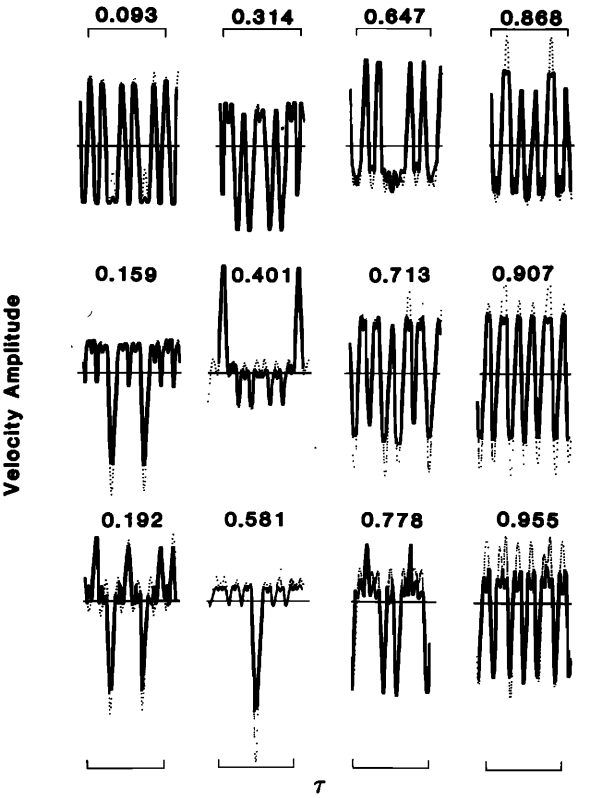

FIG. 1. Velocity waveforms of a bowed rocket wire with a bowing position of $\beta = 0.418$ obtained at the fractional observation distance δ indicated above each waveform. The vertical velocity scale is arbitrary but the same for all waveforms. The horizontal scale gives fractional time τ where one unit (indicated by the bracket) equals one period of the fundamental string vibration. The dotted curves are measurements while the solid lines are given by Eq. (3).

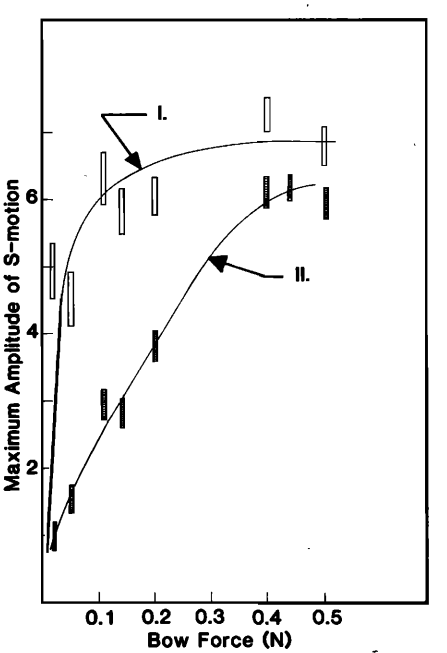

FIG. 2. Velocity amplitude (arbitrary units) of the sinusoidal part of the waveforms in S motion of a rocket wire at $\beta = 0.36$. The two curves labeled I and II show the $n = 1$ and 2 components, respectively.

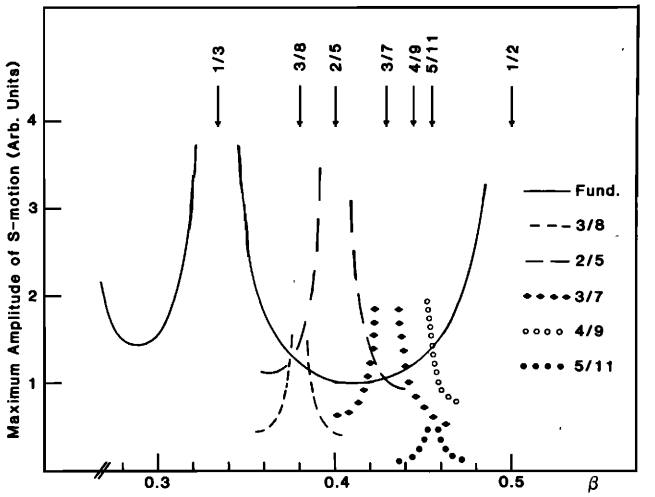

FIG. 3. Velocity amplitudes (arbitrary units) of S motion (measured and calculated) for various bowing positions near $\beta = 2/5$. Each measurement was taken at a string position where the amplitude was optimal, i.e., $\delta = \beta/2$. The solid lines are given by Eq. (3). For the sake of visual clarity the measurements have not been drawn. However, the data fell within one error bar of the solid line except near the poles. The arrows (labeled by their β values) show the positions of some poles.

tion.[4] For small forces the sinusoidal amplitude increases with increasing bow force until a plateau is reached. (The force at the onset of the plateau was used[1] to define, operationally, the critical force.) In particular, at a β value of 0.36 (see Fig. 2) the critical force for S motion occurs at a force of approximately 0.15 N whereas a bow force of 0.35 N is required to bring on harmonic S motion. Equations (1), (2), and (3) describe the motion at the plateau but not in the transition region where the bow force is less.

Asymptotically increasing amplitudes arise in normal S motion when the bowing position approaches values of $\beta = 1/m$ ($m = 1,2,3,4...$). Bowing points with $\beta = 1/m$ will be called poles. No S motion can be found there experimentally and Eq. (1) implies infinite amplitudes with kinetic energies the bow is unable to sustain.[10] Similar conditions exist in the case of higher numbered modes. For example, the second harmonic of the S motion has poles at $\beta = 2/5$, 2/7, 2/9, etc., the third harmonic at $\beta = 3/7$, 3/8, 3/10, etc. [It is convenient to discuss β values as proper fractions, e.g., $\beta = M/N$ (M and N are integers); without loss of generality we shall only consider β values on one half of the string, i.e., $M < N/2$.] Consequently, the "β versus maximum-amplitude" graph is considerably more complex here than for normal S motion.[11] The maximum amplitudes of some measurable harmonics in the region $0.36 < \beta < 0.46$ are shown in Fig. 3. [The $F(n)$ parameter was adjusted to fit the data for each harmonic.] Again, if the string is bowed very near the pole of a harmonic, the string, as a whole, fails to respond. On the other hand, if the mode in question is highly damped, the motion is well behaved even at the pole. An extreme example is provided by the normal violin string where all higher modes are, practically, unobservable and the simple Eq. (1) give good results for any $\beta \neq 1/m$ as demonstrated earlier.[12]

III. HARMONICS ON INFINITELY FLEXIBLE STRING

On lossless strings without stiffness all harmonics are undamped. One might guess that the S motion is impossible since any value of β can be thought of as lying close to a rational fraction M/N and, thus, close to poles for the Mth harmonic, indeed close to all the (MK)th harmonics ($K = 1,2,3,...$). Nevertheless, S motion may occur because, *analytically*, the amplitudes $F(MK)$ can be made zero and, *physically*, this can be justified for all higher harmonics by the finite damping of any real string. Let us first consider certain, analytically simple, waveforms. Two cases with an infinite number of harmonics in Eq. (2) or (3) are of special interest.

A. Square waveform at the bowing point

With $\delta = \beta$ in Eq. (3) the waveform at the bowing point is obtained. If an infinite number of terms are included in Eq. (3) with

$$F(n,\text{square}) = (-1)^{n+1}\frac{2\sin(\pi pn)}{\pi pn}; \quad (0<p<1), \qquad (4)$$

the velocity waveform at the bow becomes rectangular, i.e., it has a constant velocity ($= v_0$) during the sticking time and another constant velocity during the slipping time. The infinite set of parameters $F(n)$ is thereby fixed and replaced by one arbitrary parameter p (but $p < 1$), defined by $p\beta =$ slipping time at the bow point, i.e., the duration of the square wave at the bowing point. Clearly, if $p = 1/M = p(M)$ the amplitudes $F(MK,\text{square})$ are zero. This is also true if p is a multiple of $p(M)$. With such p values the poles are removed. In other words, the slipping time is quantized for square waves. It should be noted that Eq. (4) is properly normalized so that $\Sigma_{n=1}^{\infty} F(n,x) = 1$. In our model the string is assumed to be nondispersive and to have terminations which are perfect reflectors. The square wave produced at the bowing point should therefore be expected to exist anywhere on the string in various superpositions. To see if the combination of Eqs. (3) and (4) gives square waves for $\delta \neq \beta$ we must distinguish between two classes of β values.

(i) $\beta = M/N$, an irreducible rational number with M less than about seven. In this case computation shows that square waves are found everywhere on the string. For example, if $\beta = 4/9$ the value of p may be chosen as either 1/4, 2/4, or 3/4; this procedure makes every fourth term in Eq. (3) vanish, removing terms that would otherwise have been infinite. [Figure 4 shows the waveforms at the bowing point and at $\delta = 1/15$ when $p = 1/4$ with different truncations in the sum of Eq. (3).] This class of β values exhausts most of the cases considered by Raman.[5] As will be discussed later, Raman's and our waveforms generally agree.

(ii) Raman also included waveforms obtained at $\beta = r \pm e = M/N$, where r is an irreducible rational number of the type discussed in (i) and e is a small number.[13] For example, $\beta = (3/7 + e)$ might be considered equivalent to $\beta = 0.433 = 433/1000 = M/N$. Here Eqs. (2) and (4) do not give square waves even if p is chosen (e.g., $p = 200/433$) so that the poles [i.e., the 433th, the 866th, ... terms in Eq. (3)] cancel. Large terms exist below the first pole [in this case: $v(13)$, $v(29)$, $v(42)$,...] which cannot be removed by any choice

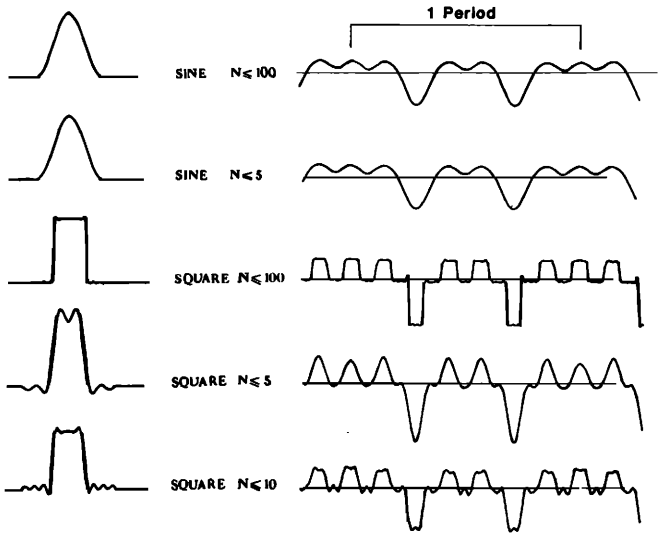

FIG. 4. Waveforms (arbitrary velocity units along the vertical direction and time along the horizontal) calculated according to Eq. (3) at bowing position $\beta = 4/9$ and measuring position $\delta = 4/9$. The summations in Eq. (3) have been terminated at the n values shown.

of p. In fact, the sum in Eq. (3) fails to converge.

The large terms occur for n values that make the denominators in Eqs. (2) and (3) small, i.e., $\sin(n\gamma) \simeq 0$. This condition arises when $n\gamma = Q\pi \pm \epsilon$ ($Q = 1,2,3,...$) or, equivalently, $n/Q = \beta \pm \chi$ (ϵ and χ are small numbers). One finds these n values by searching for rational fractions n/Q that approximate the value of β and yet have n and Q less than M and N. The algorithm for such a search can be found in the theory of continued fractions.

According to that theory[14] a rational fraction (β in this case) can be expressed by a finite continued fraction:

$$\beta = \cfrac{1}{a(1) + \cfrac{1}{a(2) + \cfrac{1}{a(3) + \cfrac{1}{\quad + \cfrac{1}{a(k)}}}}}, \tag{5}$$

where $a(1),a(2),...,a(k)$ are positive integers called partial quotients. If only $a(1),a(2),...,a(l)$ are included, one obtains the l th convergent. The convergents are, in fact, the desired approximations ($= n/Q$) to β. The lowest order convergents are

$$\beta(1) = 1/a(1),$$
$$\beta(2) = a(2)/[a(1)a(2) + 1],$$
$$\beta(3) = [a(2)a(3) + 1]/[a(1)a(2)a(3) + a(1) + a(3)].$$

This implies that terms with $n = 1$, $n = a(2)$, $n = [a(2)a(3) + 1]$ are large. {The first convergent gives a poor approximation, consequently, the denominator of the first term [$v(1)$ in Eq. (3)] is generally not close to zero.} If the irreducible fraction $\beta = M/N$, where $M < N/2 <$ about 7, Eq. (5) becomes exactly equal to β with only a few partial quotients. In that case all convergents are poor approximations except for the last which corresponds to the lowest pole [which, of course, is removed if p is chosen to be a multiple of $p(M)$]. In other words, for such β values as 3/7, 3/8, 3/10, 3/13; 4/9, 4/11, 4/13; 5/11, 5/13; 6/13 the waveform at the bowing point is a perfect square wave while the waveforms at other locations consist of line segments joined with sharp corners. On the other hand, if M and N are large, partial quotients arise which make the higher order convergents

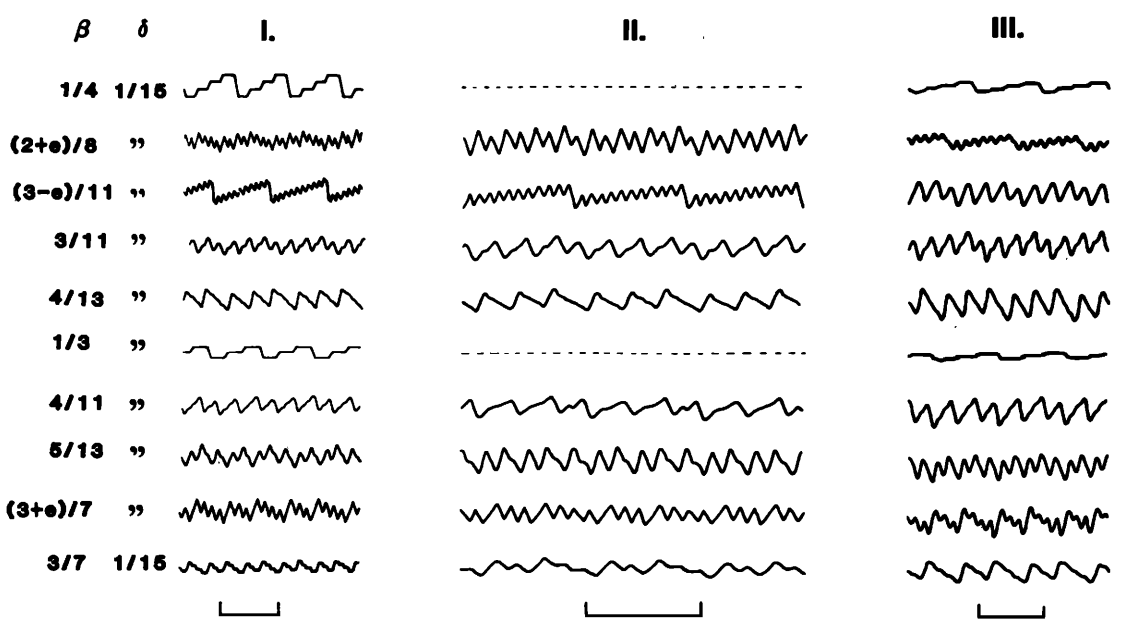

FIG. 5. Transverse deflection (arbitrary units in the vertical direction) waveforms. The horizontal direction shows time scaled to give an oscillation period of the length shown by brackets under each column. Column I: Raman's (Ref. 5, Fig. 9) waveforms; column II: waveforms given by Eqs. (2) and (6) with $p = 2/M$ where N and M are integers such that $\beta = N/M$; column III: waveforms measured on rocket wire.

close approximations to β. The numerators of these convergents give the n values of the very large terms in Eq. (3).

The values of $a(n)$ can be obtained from β by use of the *continued fraction algorithm*.[14]

It follows that the string cannot carry square waves for every value of β. To enable comparison with Raman's results, it is desirable to find a waveform (with selectable widths) that exists even when $\beta = r \pm e$ on a perfectly flexible string. Sine waves satisfy this requirement.

B. Sinusoidal waveform at the bowing point

Here we have

$$F(n,\text{sine}) = (-1)^n \frac{2\sin(\pi pn)}{\pi pn(n^2p^2-1)}; \quad (0<p\leqslant 1), \tag{6}$$

with the term $F(n = 1/p,\text{sine}) = 0$ and with the same normalization as in Eq. (4). Now the bowing point waveform alternates between the constant bow velocity during the full sticking time and a sinusoidally varying velocity during the slipping time $p\beta$. (The sinusoid goes from its maximum value through one cycle back to its maximum value in the time $p\beta$.) Again, it is necessary to remove the poles: with $\beta = M/N$, the (MK)th terms must be set to zero; this occurs when $p = 2/M, 3/M, 4/M$, etc. (If the string is bowed at the second harmonic, $\beta = 2/5,2/7,...$, this sine wave coincides with the normal S motion.) Here the minimum width, $2\beta/N$, is twice the minimum width for square waves. This implies that the full width at half maximum of the shortest sine wave has the same duration as the square wave. This is demonstrated in Fig. 4 where the two top curves (sine wave with $p = 2/4$) have the same FWHM as the curve on the third line from the top (square wave with $p = 1/4$).

Figure 4 also shows the rapid convergence of Eq. (3) for sine waves. About five terms suffice to give smooth waveforms. This is in contrast to the case of square waves where more than 100 terms are necessary. For sine waves one may put $v(n > 5) = 0$ with high accuracy and neglect poles caused by terms with $n > 5$. In that case p values are quantized for $M \leqslant 5$ (where $M/N = \beta$) but not for $M > 5$.

In this manner we can find sine wave expansions of Eq. (3) when $\beta = (r \pm e)$ since the terms that were large in the case of square wave expansion (i.e., terms with $M \geqslant 5$) now are negligibly small. Furthermore, the slipping duration $p\beta$ is not quantized in that case.

IV. COMPARISON OF RAMAN'S AND OUR WAVEFORMS

In 1891 Krigar-Menzel and Raps[15] measured 64 transverse deflection waveforms and subsequently Raman[5] presented a theory of these waveforms based on geometrical constructions. The measurements gave a few rather sharp-edged waveforms but the majority were rounded. However, Raman's method assumed a square wave at the bowing point and all his results are sharp edged. Apart from this, there is good agreement between experiment and theory with regards to relative sizes and widths of the features in the waveforms. Raman also noticed[16] the quantization of p (called ω in his work) at bowing points with $\beta = M/N$ if $M < 5$. At these points Raman assumed $p = 1/M$ in the waveforms.

Our Eq. (2) may be used to calculate the 64 waveforms. For definiteness we take sinusoidal waveforms and $p = 1/M$. At Raman's "irrational" points, i.e., $\beta = (r \pm e)$, p is chosen near the values that would be used at $\beta = r$. These waveforms are in good agreement with the measurements[15] and a comparison with a typical set of Raman's waveforms is shown[17] in Fig. 5. The only exception to the agreement is the third waveform from the top which will be discussed below.

V. HARMONIC S MOTION IN GENERAL

In reality, as the data in Fig. 1 shows, the waveform at the bowing point (or, equivalently, at $\delta = 1 - \beta$) is neither a square wave nor a sine wave. The data of Krigar-Menzel and Raps[15] did not clearly show this and Raman,[5] simply, assumed that the waveforms were square at the bow point.

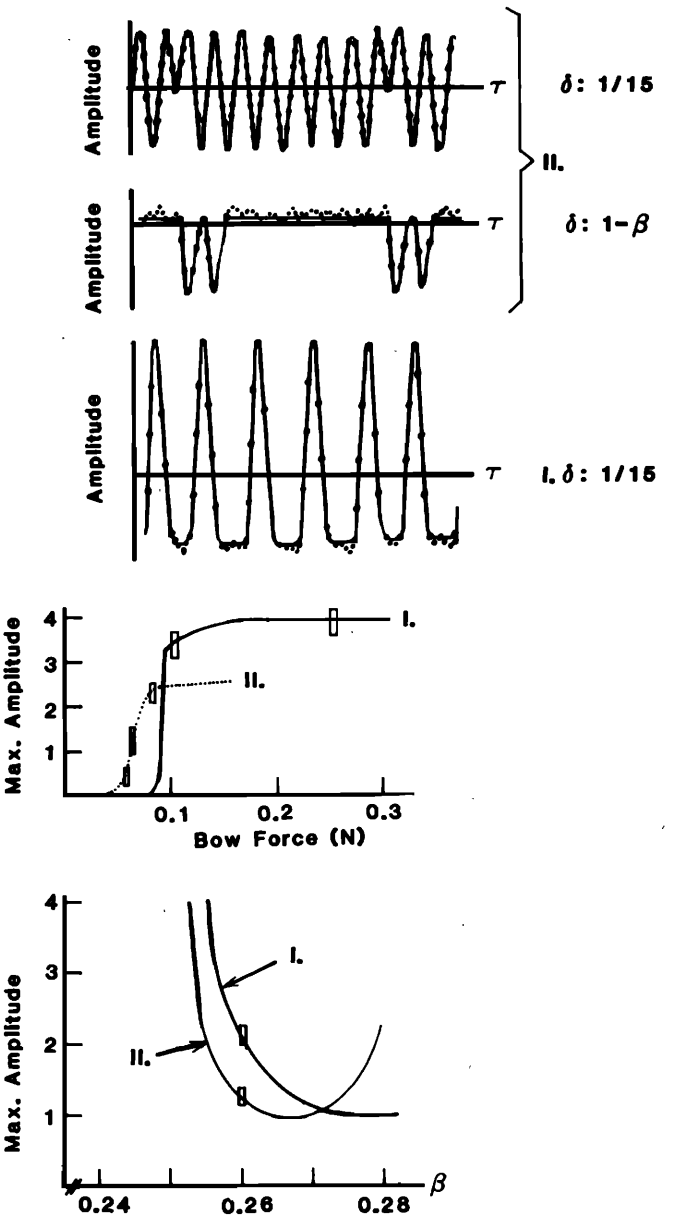

FIG. 6. Various measurements (dots and boxes) and calculations (solid lines) pertinent to the second waveform (from the top) of column III in Fig. 5. In all cases the vertical axes show transverse velocities proportional to the values given by Eq. (3) when relevent F values are unity.

Occasionally our measurements give rather peculiar waveforms at the bowing point. The second waveform from the top in Fig. 5 (column III) is measured at a β value slightly above the $\beta = 1/4$ pole; each cycle shows 11 small peaks superposed on a ramp. The waveform can be generated by Eq. (2) if one takes $F(1) = F(n > 2) = 0$ and $F(2) = 1$, i.e., the fundamental is suppressed. Figure 6 shows the corresponding velocity waveforms at $\delta = 1/15$ (11 peaks/cycle) and at the bowing point (a W shape during the slipping time). These results occur at a moderate bowing force (about 0.075 N). With larger force (about 0.11 N) the fundamental of the S motion dominates as shown in the third waveform (from the top) in Fig. 6. The reason this happens can be learned from the two lower curves: at this point ($\beta = 0.26$) the harmonic ($n = 2$) of the S motion can be elicited at a lower bow force than the fundamental ($n = 1$).

VI. CONCLUSIONS

Equations (2) and (3) account for all observed waveforms produced by sufficiently large bow force (0.02 to 0.4 N depending on the value of β) and sufficiently large β (> 0.18). Most violin strings are thick enough to prevent the formation of harmonics in which case Eq. (3) reduces to Eq. (1). For more flexible strings the harmonics come into play. If a highly flexible string is bowed at $\beta = M/N$, the (KM)th term in Eq. (2) or (3) (i.e., at the pole) becomes very large and the expansion in the equations fail to converge. S motion may still be possible at such points if $F(KM) = 0$ in which case the pole is cancelled. (For real strings of some thickness this situation probably implies that all harmonics with $n > M$ are damped out as well.) Very flexible strings permit high harmonics and they are, thus, difficult to bow at "rational" points (where $\beta = M/N$ with low M values).

Another way to cancel the poles is to assume that the waveform is square (as Raman[5] did) but the F values must then be arranged in specific ways [i.e., according to Eq. (4)] that are unlikely to occur experimentally. Real strings are more likely to have rounded (e.g., sinusoidal) waveforms because the harmonic content drops off fast [as n^{-3}, see Eq. (6), provided p is not too small]. Both square and sinusoidal waveforms may give S motion even when a very flexible string is bowed at a "rational point" ($\beta = M/N$) if the duration of the slipping time is quantized to values that are multiples of β/N.

[1]B. Lawergren, "On the motion of bowed violin strings," Acustica **44**, 194–206 (1980).

[2]B. Lawergren, "A new and a rediscovered type of motion of the bowed violin string," Catgut Acoust. Soc. Newslett. **30**, 8–13 (1978).

[3]H. L. F. Helmholtz, *On the Sensations of Tone as a Physiological Basis for the Theory of Music*, translated by A. J. Ellis from the German edition of 1877 (Longmans, Green and Co., London, 1895; reprinted by Dover), Appendix VI.

[4]See Ref. 1, Figs. 4, 9, and 10.

[5]C. V. Raman, "On the mechanical theory of bowed strings and of musical instruments of the violin family, with verification of results," Proc. Indian Assoc. Advance. of Sci. **15**, 1–158 (1918), Figs. 9–12.

[6]Servodisc™ motor made by PMI Motors, 5 Aerial Way, Syosset, NY.

[7]Supplied by Super Sensitive String Co., R.R. 4, Box 30-V, Sarasota, FL 33577.

[8]Model 805, Biomation, Cupertino, CA 95014.

[9]The equation for harmonic S motion suggested earlier [Ref. 1, Eq. (5)] is incorrect since it does not account for the observed poles although it may give some waveforms with fair degree of accuracy, see Fig. 19, Ref. 1. Detailed experimental study of β dependence near the second harmonic at $\beta = 2/5$ shows that Eqs. (2) and (3) are correct.

[10]However, waveforms without S motion can be obtained at $\beta = 1/m$ if the bowing force is very small. This results in Helmholtz motion [i.e., the non-sinusoidal part of Eq. (1)] with a missing (total string) harmonic, namely the one with a node at the bowing point, i.e., the mth harmonic.

[11]See Ref. 1, Fig. 5.

[12]See Ref. 1, Figs. 12 and 13.

[13]We use Raman's (Ref. 5) notation of e instead of the usual ϵ.

[14]G. H. Hardy and E. M. Wright, *An Introduction to the Theory of Numbers* (Oxford U. P., London, 1938), Chap. 10.

[15]O. Krigar-Menzel and A. Raps, "Ueber Saitenschwingungen," Berl. Klin. Preuss. Akad. Wiss., Sitzungsber. **44**, 613–629 (1981).

[16]See Ref. 5, Figs. 13–15.

[17]See Ref. 2, Fig. 9 which includes the waveforms of Raman, Ref. 5, Fig. 9.